

Experimental investigation of X-ray spectral absorption coefficients in heated Al and Ge on the Iskra-5 laser facility

S.V. Bondarenko, R.V. Garanin, N.V. Zhidkov, A.V. Pinegin, N.A. Suslov

Abstract. We set forth the data of experimental investigation of X-ray spectral absorption coefficients in the 1.1–1.6 keV photon energy range for Al and Ge specimens bulk heated by soft X-ray radiation. Two experimental techniques are described: with the use of one facility channel and the heating of specimens by the X-ray radiation from a plane burnthrough target, as well as with the use of four channels and the heating by the radiation from two cylindrical targets with internal input of laser radiation. The X-ray radiation absorption coefficients were studied by way of transmission absorption spectroscopy using backlighting X-ray radiation from a point source. The results of investigation of X-ray spectral absorption coefficients on the 1s–2p transitions in Al atoms and the 2p–3d transitions in Ge atoms are presented.

Keywords: X-ray radiation path lengths, X-ray backlighting, absorption spectroscopy, laser plasma.

1. Introduction

Investigation of the spectral absorption coefficients for X-ray radiation (XR) in heated materials is among the problems of plasma physics which are extensively studied theoretically and experimentally. Determining the XR absorption coefficients in targets of different type is critically important to their subsequent use. To theoretically simulate the absorption coefficients will require learning the detailed structure of the atoms, the energy level populations and the shapes of spectral lines with the inclusion of multiparticle interactions in the plasma. This results in that the existing numerical-theoretical models are bound to rely on several approximations, which call for experimental verification. That is why in several countries the experimental investigations of XR absorption coefficients in heated materials are carried out using different heating soft-XR sources based on a laser-produced plasma [1–5] or a z-pinch [6]. These investigations are performed both for transitions to the K shell, which nowadays are turning more into a means of temperature measurement for the material under heating rather than into a subject of study, and for transitions to the L shell [7, 8] and even to the M shell [9] in a relatively broad temperature range – from several tens of electronvolts to ~ 160 eV [6].

S.V. Bondarenko, R.V. Garanin, N.V. Zhidkov, A.V. Pinegin, N.A. Suslov
Russian Federal Nuclear Centre – ‘All-Russian Research Institute of Experimental Physics’, prosp. Mira 37, 607190 Sarov, Nizhniy Novgorod region, Russia; e-mail: suslov@otd13.vniief.ru

Received 13 September 2011, revision received 26 October 2011
Kvantovaya Elektronika 42 (1) 51–57 (2012)
Translated by E.N. Ragozin

In our paper we describe the techniques of experiments and outline the results of investigations of the spectral XR absorption coefficients in the $h\nu \sim 1.1–1.6$ keV energy range for Al and Ge specimens heated by soft XR. The experiments were carried out on the Iskra-5 iodine laser facility [10].

The spectral absorption coefficients were investigated by the method of absorption spectroscopy with the employment of a backlighting point XR source, which furnished the possibility of comparing – in one experiment and under similar conditions – the spectra of the XR transmitted through the layer of material under study and of the XR passed by it [11]. The material layer was backlit with a certain delay relative to the instant of its heating, which permitted selecting the state of the heated layer.

We describe experiments carried out with the use of either one or five facility channels. Also presented are the technique and the results of experiments aimed at evaluation of the density of the heated Al layer.

2. Design of specimens with a layer of material under investigation

The specimens intended for the investigation of XR absorption coefficients were a thin material layer of thickness $t \sim 0.1$ μm confined between two CH-plastic films of thickness ~ 1 μm each. The CH films moderated the expansion of the heated material layer, ensured its higher densities ρ , and minimised its density gradient over the layer thickness. The layer of material under investigation occupied only one half of the aperture of this sandwich made up of the CH films and the layer confined between them, the other half consisted only of two CH film layers. The backlighting XR transmitted through the material-free part of the sandwich aperture experienced only a weak absorption, while the radiation transmitted through the part of the aperture with the material layer experienced a stronger absorption. The use of a point backlighting XR source permits us to distinguish the spectra of radiation transmitted through different parts of the sandwich and to compare them for determining the spectral absorption coefficients.

The layer thicknesses were interferometrically measured with ‘witnesses’ fabricated simultaneously with the working layers. The uncertainty of thickness measurements for numerical processing of interferograms was equal to ~ 0.01 μm .

To check the correctness and consistency of the measurement data (the use of correct characteristic curve of X-ray photographic film to convert optical densities to XR exposures, the inclusion of the contribution of background radiation, uniform state distributions of the heated layer, its density, temperature, and ionisation state over the surface and depth of the layer under investigation) we also fabricated three-zone

specimens containing Al layers with different thicknesses (0.1 and 0.05 μm) in the outer zones, the central, reference, zone consisting of only the double CH layer in this case. Under ideal conditions, the absorption coefficients determined for these layers must coincide on being reduced to the same thickness.

The spectral XR absorption coefficients in Al are theoretically described with reasonable accuracy. More arduous for numerical simulations are ions with higher charges Z and, as a consequence, with a more complex structure of energy levels and a huge number of transitions between them. The simplest of such transitions are those to the L shell. In this connection, experimental investigations of XR absorption coefficients are carried out in materials like Fe, Ni, Ge, and Nb [12–15]. The material most suited to our conditions is Ge, and so specimens with a Ge layer were fabricated for the investigation of XR absorption coefficients along with the specimens with an Al layer.

Another specimen was prepared for determining the heated layer density. According to numerical simulations with the use of the one-dimensional gas-dynamic SNDP program [16], by the instant of probing the Al-layer thickness increases by a factor of ~ 135 ; for its initial thickness of 0.1 μm this gives 13.5 μm . This thickness is too small to be precisely measured. At the same time, numerical simulations suggest that thicker layers are also heated to the same temperatures as the thin ones under our experimental conditions. That is why the thickness of Al layer was increased to $\sim 0.2 \mu\text{m}$ for the experiment to measure its density in the heated state; the dimension in the probing direction was equal to 100–150 μm . The aluminium layer was also sealed between CH tampers $\sim 1 \mu\text{m}$ thick each.

3. Setup of experiments with the use of one facility channel

Figure 1 shows the experimental setup with the use of one facility channel [17]. The laser radiation (LR) of one of facility channels was converted to the second harmonic and used to irradiate a converter target. The X-ray radiation produced by the converter heats a specimen with the layer of the material under investigation. The fundamental frequency radiation remaining upon conversion to the second harmonic is used to

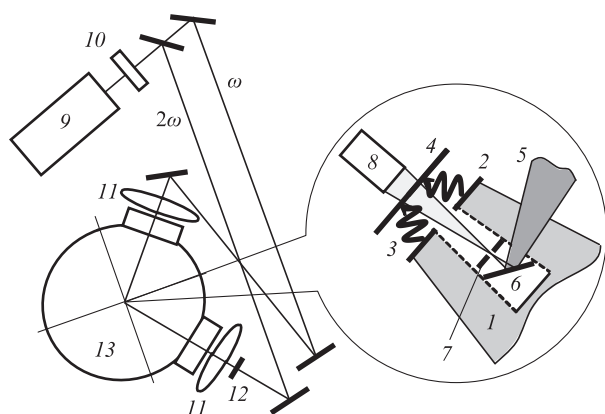


Figure 1. Experimental setup for investigating XR absorption coefficients with the use of one facility channel: (1) laser beam at a frequency 2ω ; (2) converter; (3) heating XR flux; (4) layer of material under investigation; (5) laser beam at a frequency ω ; (6) target for generating an X-ray backlighting pulse; (7) point-like aperture; (8) spectrograph; (9) final LR amplifier; (10) crystal converter; (11) focusing lenses; (12) non-transparent screen; (13) vacuum chamber.

generate the source of XR for backlighting the specimen under study. The converter was a thin, burnthrough, gold layer ($\sim 0.1 \mu\text{m}$) deposited on a 0.5–1 μm thick CH plastic film.

The scheme of X-ray backlighting was so organised that the probing XR beam propagated coaxially with the ‘power’ LR. This permitted minimising the separation of the converter target from the sample under investigation and maximising the heating XR flux. A hole 400 μm in diameter was made at the centre of the converter to avoid attenuation of the probing XR by the converter material and obviate its background radiation. The central part of the power beam was shut with a screen to prevent the LR from impinging on the specimen. Our estimates suggest that it is possible to obtain a sufficiently lengthy region with a relatively uniform XR illumination for a certain separation of the converter from the specimen under investigation.

To produce a point source of backlighting XR, use was made of an additional plane target with a rather large irradiation spot in combination with an aperture stop with a small opening 100–150 μm in diameter; in this case, the spectral resolution was high enough to resolve the absorption bands corresponding to ions with different degrees of ionisation. The target of the backlighting XR source was made of dysprosium, whose emission spectrum contained a rather bright band in the spectral range of interest ($h\nu \sim 1.5 \text{ keV}$). A flat KAP crystal spectrograph was employed to analyse the backlighting XR spectrum. To determine the energy scale on the spectrograms, a narrow strip of foil of suitable material, of aluminium in this case, was placed in front of the photographic film in the spectrograph. From the known energy of the photoabsorption edge in the foil material this enabled us to determine the energies of spectral components, including absorption lines, recorded in the spectrograms. The XR spectra were recorded on UF-4 X-ray photographic film.

The thicknesses of the layer of the material under investigation and the CH layers as well as the optimal instant of backlighting were selected proceeding from numerical simulations with the use of the SNDP code. Calculated at the first stage were the characteristics of soft XR inside the radiation source and at the specimen under investigation. Calculated next were the dynamics of specimen heating as well as the density and temperature profiles at different points in time.

The transmission coefficient τ was determined by the formula

$$\tau(h\nu) = \frac{I_{\text{layer}}(h\nu) - I_{\text{b}}(h\nu)}{I_{\text{ref}}(h\nu) - I_{\text{b}}^*(h\nu)}, \quad (1)$$

where I_{layer} and I_{ref} are the XR intensities on the spectrogram, which correspond to the radiation transmitted through the layer of the material under investigation and the radiation transmitted past it; I_{b} and I_{b}^* their corresponding background intensities on the photographic film beyond the spectrographic image in the vicinity of a given spectral range. To convert optical densities to XR intensities, use was made of the characteristic curve of UF-4 X-ray photographic film obtained at the Al K_{α} emission line with a photon energy $h\nu \approx 1.49 \text{ keV}$, which is close to the photon energy in the domain under investigation.

4. Setup of experiments with the use of five facility channels

When an Al specimen was to be heated to a temperature above $\sim 25 \text{ eV}$, the investigations of XR absorption coeffi-

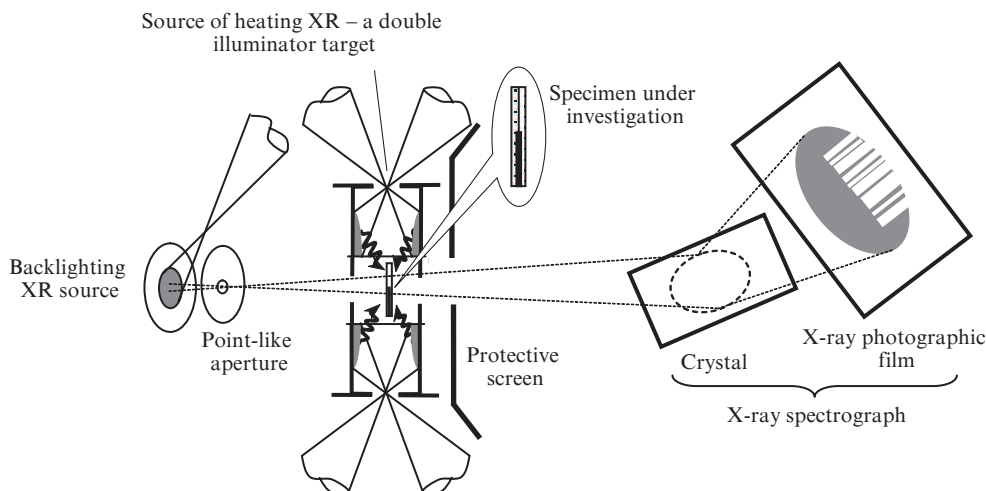


Figure 2. Schematic representation of experiments aimed at the investigation of XR paths on the Iskra-5 laser facility.

cients were carried out in the multichannel chamber of the Iskra-5 facility with the use of five channels: four channels were used to produce the heating XR and the fifth one was used to produce the probing XR. Figure 2 is a schematic diagram of the experiments.

To produce the heating soft XR in experiments on the multichannel chamber, use was made of a double illuminator target, which is qualitatively similar to the targets described in Refs [14, 15]. This target consists of two coaxial cylindrical illuminator targets and a central, diagnostic, box located between them. The two similar illuminators arranged symmetrically provide a uniform heating of a specimen throughout its surface. The specimen with a layer of the material under investigation was mounted either on the side surface of the diagnostic box or inside of it (realised in this case was a more depth-uniform two-sided heating of the specimen).

The diameters of the illuminators and of the diagnostic box were the same and equal to 1 mm, the lengths of the illuminators ranged between 1 and 1.2 mm, and the diagnostic box ranged in length between 1 and 1.6 mm. The laser radiation was injected into the illuminators through the openings in either their end faces (two LR beams through each opening) or in their side walls (one beam through each of the four openings).

The illuminator and diagnostic box bodies were made of CH plastic. To achieve a high LR-to-soft XR conversion efficiency, the inner surfaces of the illuminators and the diagnostic cell were coated with a layer of gold. The diagnostic cell was separated by a thin gold-coated CH film from the illuminators.

Two beams of second-harmonic LR each with an energy of 200–250 J and a pulse duration $\tau_{0.5} \sim 0.6$ ns were injected into each illuminator. To transmit the probing XR, either round or square openings were cut in the diagnostic box. As before, the layer of material under investigation was sealed between two CH plastic films each ~ 1 μm in thickness. The material layer occupied one half of the aperture area of the opening for backlighting radiation.

To analyse the spectrum of the backlighting XR transmitted through a specimen, we employed a spectrograph with a flat KAP crystal ($2d = 26.63$ \AA); in this case, the spectral resolution was equal to 2–2.5 eV, depending on the source size defined by the point-like aperture. In several experiments with a specimen with an Al layer, use was also made of a PET crystal ($2d = 8.742$ \AA) spectrograph. To achieve the requisite width

of spectral range, the PET crystal was bent to a cylinder of radius ~ 80 mm. The spectral resolution of this spectrograph amounted to ~ 0.5 eV.

To protect the photographic film from background radiation, between the targets and the spectrograph we placed a protective screen with an opening for observing the specimen under investigation.

5. Setup of experiments to determine the density of a heated specimen

Apart from experiments to measure XR absorption coefficients, we also carried out experiments to determine the density of a heated Al layer by measuring its thickness, like in Ref. [18].

Figure 3 shows the setup of experiments aimed at determining the thickness of a heated Al layer; this setup is largely similar to the setup intended for measuring XR absorption coefficients. To obtain spatial resolution, we placed a 20- μm wide slit in front of the input window of the spectrograph; in this case, for a magnification $M = 3$ the spatial resolution is $\Delta r = 27$ μm , which is comparable with the expected thickness of the heated Al layer, and so it may be determined with sufficient accuracy. The point-like aperture previously employed for achieving a high spectral resolution was not used in these experiments because of the requirement of obtaining a suffi-

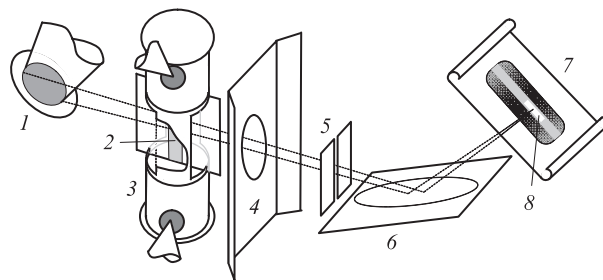


Figure 3. Setup of the experiment to determine the thickness of a heated specimen: (1) XR backlighting source; (2) narrow strip of the layer of the material under investigation; (3) illuminator target; (4) protective screen; (5) slit in the spectrograph which introduces spatial resolution; (6) KAP crystal; (7) X-ray photographic film; (8) shadow image of the layer under investigation formed in the absorption line.

ciently high photometric density in spectrograms. In this case, the spectral resolution was determined by the total visible size of the XR source and was equal to ~ 15 eV.

The LR energy injected into the illuminators in the experiment to determine the heated Al layer density was equal to ~ 700 J for a probing radiation delay of 0.75 ns.

5.1. Results of experiments with the use of one facility channel

In this case, the investigation of XR paths was carried out with an Al layer. The energy of LR at the converter was equal to ~ 170 J, the Al layer thickness was $0.15 \mu\text{m}$, the thickness of one of CH layers was equal to $1.25 \mu\text{m}$ and the thickness of the other to $0.6 \mu\text{m}$. The delay between the backlighting and heating XR pulses was equal to ~ 0.5 ns.

A spectrogram recorded in the experiment and the result of its processing are depicted in Fig. 4, where three absorption lines are clearly visible. The spectral mark on the spectrogram corresponding to the aluminium absorption K-edge permits determining the energies of the recorded absorption lines. According to the literature data, these lines correspond to the 1s–2p transitions of Al ions with different degrees of ionisation 4–6 [19].

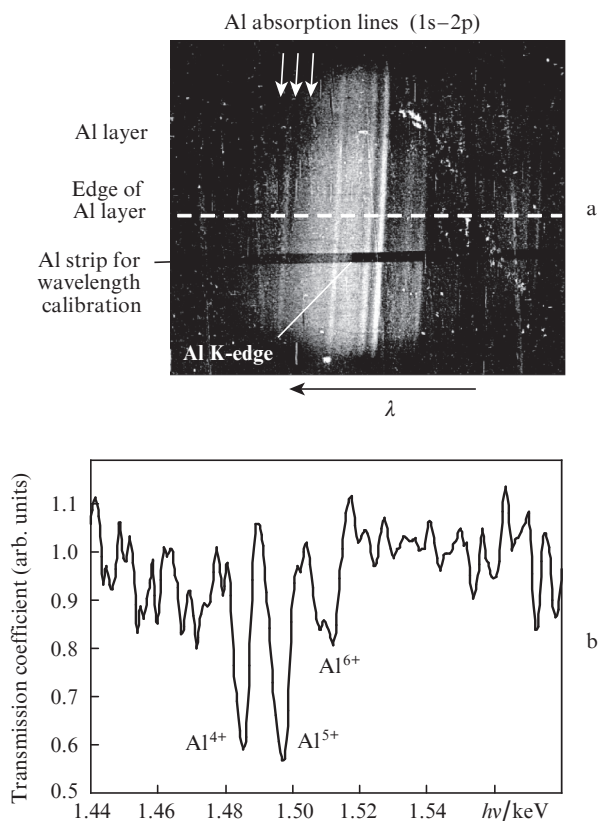


Figure 4. Results of the measurement of XR absorption in heated aluminium: spectrogram of backlighting XR from a Dy target (a) and transmission coefficient of a heated Al layer (b).

Assuming that ρt for heated Al is the same as for cold Al, we conclude that the depth-average absorption coefficient of heated aluminium, for instance on the Al^{5+} ion line, is equal to $1.3 \times 10^4 \text{ cm}^2 \text{ g}^{-1}$, which is approximately 30 times higher than for cold aluminium ($4.03 \times 10^2 \text{ cm}^2 \text{ g}^{-1}$ [20]).

According to our simulations, at the instant of backlighting pulse action the temperature in the specimen amounted to ~ 25 eV and the average degree of ionisation was equal to 4 and higher, which is consistent with the data of the experiments performed here.

5.2. Results of experiments with the use of several facility channels

In this case, the investigation of spectral XR absorption coefficients in aluminium was performed with a specimen with a $0.1\text{-}\mu\text{m}$ thick Al layer; the CH tampers each were $1 \mu\text{m}$ thick. The energy of LR injected into the illuminators was equal to ~ 700 J for pulse durations $\tau_{0.5} \sim 0.5$ ns. The specimen was mounted on the side surface of the diagnostic box. The probing radiation was delayed by 0.75 ns. The spectrograph with a flat KAP crystal had a spectral resolution of 2.3 eV. An experimentally recorded spectrogram and the results of its processing are given in Fig. 5.

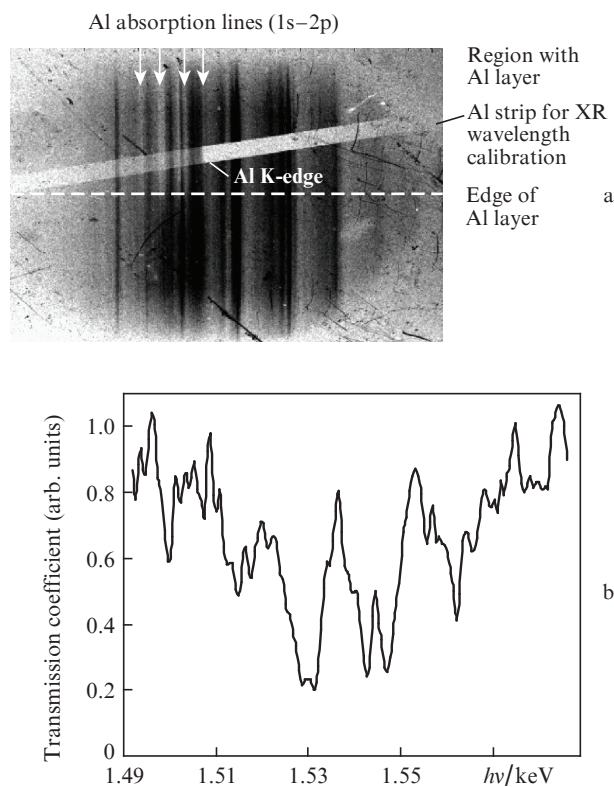


Figure 5. Results of measurement of the XR absorption in a specimen with a $\sim 0.1 \mu\text{m}$ thick Al layer placed on the side surface: spectrogram (a) and transmission coefficient of the heated Al specimen (b).

The absorption lines arising from 1s–2p transitions are clearly visible in the spectrogram. According to our simulations, the average Al layer temperature in this experiment is equal to 46 eV for a specimen heating nonuniformity of $\sim 10\%$; the lowest and highest densities differ by about 20%.

We also carried out experiments with an aluminium specimen using a PET crystal spectrograph with a spectral resolution of ~ 0.5 eV to record the spectrum. A specimen with an $0.11\text{-}\mu\text{m}$ -thick Al layer was placed inside the diagnostic box. The energy of LR injected into the illuminators was equal to ~ 900 J; the probing radiation delay was equal to 0.7 ns.

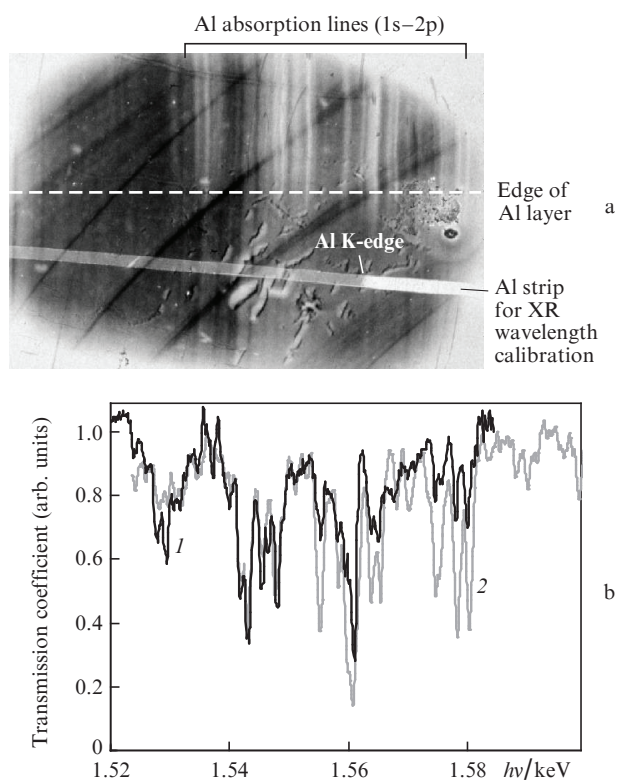


Figure 6. Results of the XR absorption measurement with a high spectral resolution in the experiment with an Al specimen mounted inside the diagnostic box: spectrogram (a) and transmission coefficients of a heated Al layer obtained in experiments on the Iskra-5 facility (1) and on the Nova facility [21] with a 0.05- μm thick Al layer specimen (2) (b). Curve (1) was re-calculated for a 0.05- μm layer thickness.

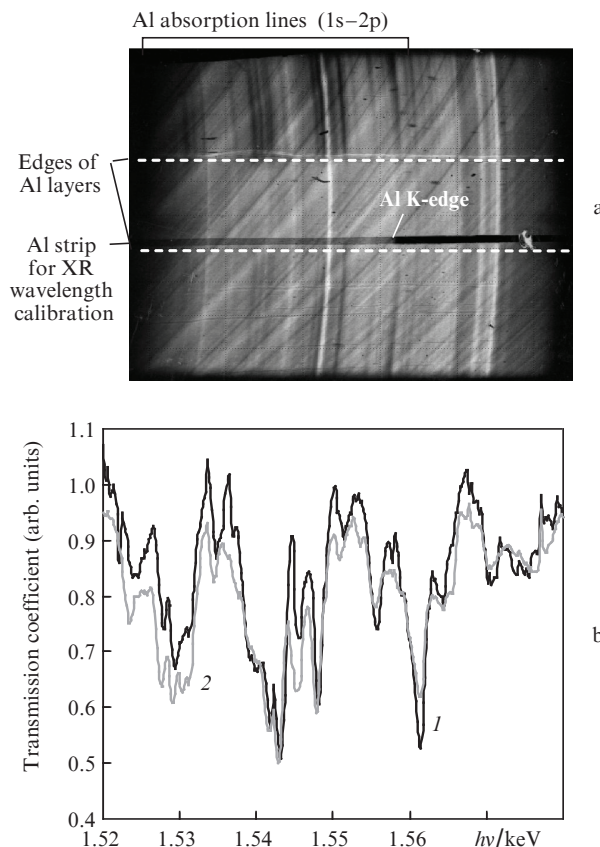


Figure 7. Results of the XR absorption measurement in a specimen with two Al layers: spectrogram (a) and transmission coefficients of heated Al layers 0.05 (1) and 0.1 μm (2) in thickness (b). Curve (2) was calculated for a 0.05- μm layer thickness.

The recorded spectrogram and the results of its processing are presented in Fig. 6. The absorption lines arising from 1s–2p transitions and their detailed structure are clearly seen in the spectrogram. To compare with the data of Ref. [21], the measured transmission coefficients were re-calculated for a layer thickness of 0.05 μm . The results of that work are often used for comparison with the data of numerical-theoretical simulations.

The temperature of the specimen in Ref. [21] is estimated at 58 eV and the density at 0.02 g cm⁻³, which is close to our experimental conditions. One can see that the spectral components recorded on the Iskra-5 facility are in rather good agreement with those presented in Ref. [21]. It is also evident that the strongest absorption lines observed in our experiment lie in a softer spectral region, and the temperature was therefore somewhat lower.

Figure 7 shows the results of an experiment with a specimen which had two aluminium layers of different thickness. The specimen was placed inside the diagnostic box; the layer thicknesses were equal to 0.05 and 0.1 μm . The energy of LR injected into the illuminators was equal to ~ 600 J for a probing radiation delay of 0.6 ns. The spectral resolution of the spectrograph was equal to ~ 0.5 eV.

In the spectrogram one can clearly see two zones corresponding to aluminium layers of different thickness, which contain the absorption lines arising from 1s–2p transitions. The spectral absorption coefficients obtained for the different thicknesses are reduced to the same thickness (0.05 μm) for clarity; the coefficients are seen to be in reasonably close agreement. In our opinion, some visible difference between

the coefficients is attributable to the noise due to nonuniform reflection from the crystal as well as to the insufficient brightness of backlighting XR in some spectral regions. One can also see from Fig. 7 that the absorption lines shifted to the softer domain with a decrease in LR energy injected into the illuminators, which testifies to a lowering of the temperature of the layers under investigation.

In the investigation of XR absorption coefficients in germanium, the specimen was a 0.14- μm -thick Ge layer confined between CH plastic layers each 0.9 μm thick. The specimen was mounted inside the diagnostic box. The energy of LR injected into the illuminators was equal to ~ 900 J for a probing radiation delay of 0.6 ns. The spectral resolution was equal to ~ 2.5 eV. The target intended for the generation of backlighting XR was made of neodymium.

The results of experiment with the germanium specimen are depicted in Fig. 8. The spectrogram shows an absorption band arising from 2p–3d transitions. A comparison of the energies of the components of the spectral absorption coefficients recorded in our experiment with the simulations of Ref. [22] allows a conclusion that the temperature of the heated Ge layer in the experiment was equal to ~ 30 eV.

5.3. Results of experiments to determine the thickness of heated aluminium layer

Figure 9 shows the spectrogram with the shadow image of the specimen with an aluminium layer and the results of its processing. We emphasise that aluminium heated to several tens

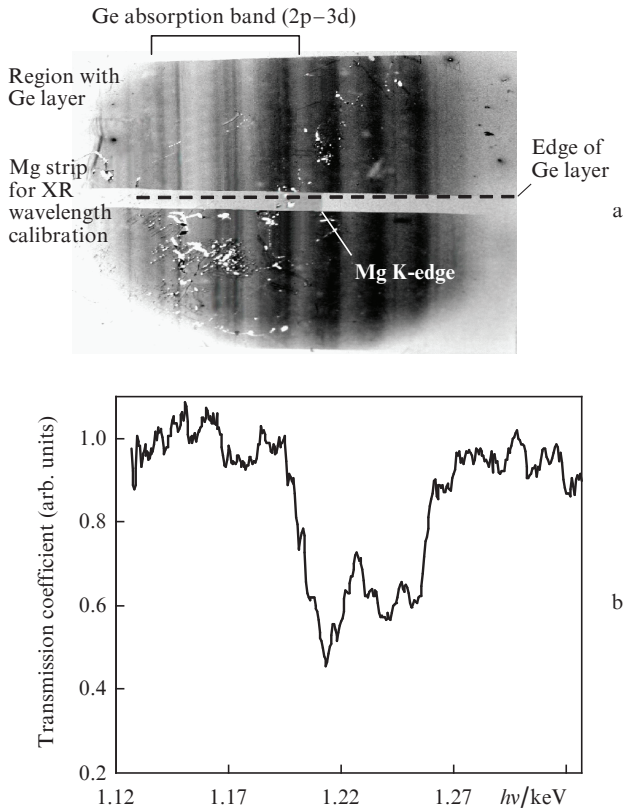


Figure 8. Results of the XR absorption measurement in a specimen with a $0.14\text{-}\mu\text{m}$ thick Ge layer under two-sided heating: spectrogram (a) and transmission coefficient of the heated Ge specimen (b).

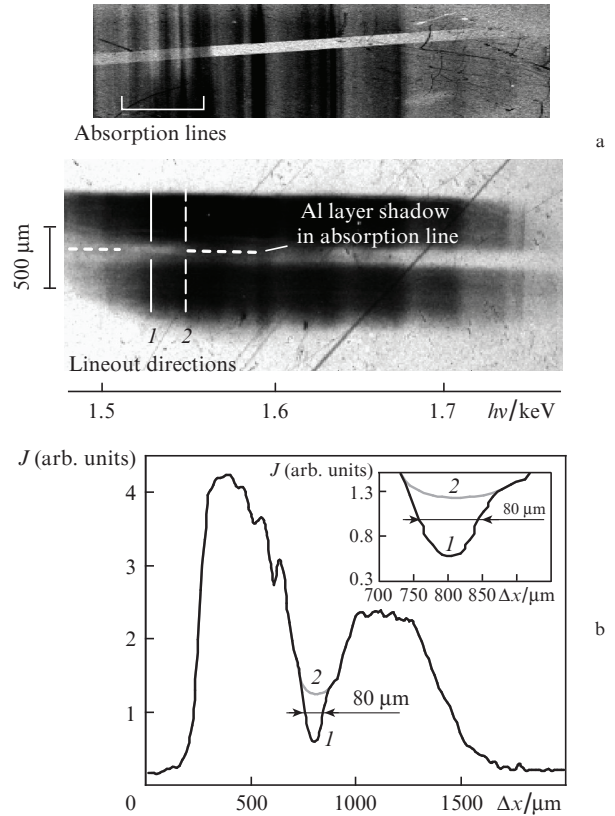


Figure 9. Spectrogram with the shadow image of a film with an aluminium layer (a) and lineouts of the spectrogram in the region of absorption lines (1) and outside of this region (2) (b).

of electronvolts absorbs the probing radiation only in the region of absorption lines and remains virtually transparent for the rest of the energies, and the shadow image of the heated material may therefore be obtained in the energy range corresponding to the absorption lines. In the experiment to determine the thickness of heated Al layer, the spectral resolution is low due to the absence of a point-like aperture. That is why for clarity in Fig. 9a we give the spectrogram with absorption lines recorded with a high spectral resolution in the experiment to investigate XR paths. Comparing the spectrograms shows that the spectral position of the domain where the shadow picture of the heated aluminium layer is observed agrees nicely with the position of absorption lines in the spectrogram with a high spectral resolution, which is indicative of the recording of the shadow image of heated Al layer in the absorption lines.

A lineout of the spectrogram with the shadow image of Al layer taken along the absorption line is given in Fig. 9b. One can see that the absorption region is bell-shaped and its width is equal to $80\text{ }\mu\text{m}$. A comparison of the lineout with the calculated profiles of the shadow images of a domain with a Gaussian absorption profile of different width, with the recording of these images with the aid of a $20\text{-}\mu\text{m}$ -wide slit aperture with a magnification $M = 3.2$ (as under our experimental conditions), suggests that the Al layer thickness in our experiment at the instant of probing was equal to $14 \pm 3\text{ }\mu\text{m}$. Consequently, for an initial layer thickness of $0.24\text{ }\mu\text{m}$ the heated layer density was equal to $(4.6 \pm 1.0) \times 10^{-2}\text{ g cm}^{-3}$ at the instant of probing.

According to the data of our numerical simulations, at the point in time $\Delta t = 0.7\text{ ns}$, which is close to the instant of prob-

ing, the electron temperature of aluminium plasma layer is equal to 65 eV and its density is equal to $2.34 \times 10^{-2}\text{ g cm}^{-3}$. The experimentally determined density of the heated Al layer is approximately two times higher than the value calculated for a close point in time. It is pertinent to note that the energy of LR injected into the illuminators was assumed to be equal to 900 J in our simulations, which was greater than the corresponding energy in our experiments, and so the specimen is more intensely heated and its density should be lower. Therefore, the experimentally determined density of the heated aluminium specimen is in satisfactory agreement with its calculated value.

A comprehensive description of our numerical simulation of the layers under heating and a comparison of the calculated spectral absorption coefficients with experimental data will be presented elsewhere.

6. Conclusions

Therefore, we have developed an experimental technique for investigation the spectral XR absorption coefficients for materials bulk-heated by soft XR.

We made targets and carried out experiments with thin-film Al and Ge specimens $0.05\text{--}0.15\text{ }\mu\text{m}$ in thickness. In the spectral range $h\nu \sim 1.1\text{--}1.6\text{ keV}$, absorption lines arising from the $1s\text{--}2p$ transitions in Al and the $2p\text{--}3d$ transitions in Ge were recorded.

In additional experiments, the density of an aluminium specimen heated to a temperature of $\sim 65\text{ eV}$ was measured to be equal to $(4.6 \pm 1.0) \times 10^{-2}\text{ g cm}^{-3}$.

The elaborated experimental technique and method for measuring absorption spectra permit investigating XR paths in materials bulk heated by soft XR on the Iskra-5 laser facility.

Acknowledgements. The authors express their appreciation to S.G. Garanin, G.G. Kochemasov, S.A. Bel'kov, and A.V. Bessarab for their constant interest in the work and helpful discussions, to V.M. Izgorodin and B.S. Zimalin for their help in fabricating the elements of targets, to M.A. Barinov, V.F. Ermolovich and V.A. Karepov for numerical simulations of the experiments, to O.O. Sharov for presenting the data of preliminary calculations, to V.I. Annenkov, S.V. Kalipanov, V.P. Kovalenko, A.G. Kravchenko, V.A. Krotov, S.I. Petrov, and G.V. Tachaev, as well as to the whole team of the Iskra-5 laser facility for the preparation and pursuance of experiments.

References

1. Perry T.S., Budil K.S., Cauble R., et al. *J. Quant. Spectr. Rad. Transfer*, **54**, 317 (1995).
2. Eidmann K., Schwanda W., Foldes I.B., et al. *J. Quant. Spectr. Rad. Transfer*, **51**, 77 (1994).
3. Foster J.M., Hoarty D.J., Smith C.C., et al. *Phys. Rev. Lett.*, **67**, 3255 (1991).
4. Chenais-Popovics C., Gilleron F., Fajardo M., et al. *J. Quant. Spectr. Rad. Transfer*, **65**, 117 (2001).
5. Baohan Zhang, Guohong Yang, Wenhai Zhang, et al. *Phys. Plasmas*, **9**, 678 (2002).
6. Bailey J.E., Rochau G.A., Iglesias C.A., et al. *Phys. Rev. Lett.*, **99**, 265002 (2007).
7. Chenais-Popovics C., Merdji H., Missalla T., et al. *The Astrophys. J. Suppl. Ser.*, **127**, 275 (2000).
8. Hoarty D.J., Harris J.W.O., Graham P., et al. *High Energy Density Physics*, **3**, 325 (2007).
9. Merdji H., Mißalla T., Blenski T., et al. *Phys. Rev. E*, **57**, 1042 (1998).
10. Annenkov V.I., Bagretsov V.A., Bezuglov V.G., et al. *Kvantovaya Elektron.*, **18**, 536 (1991) [*Sov. J. Quantum Electron.*, **21** (5), 487 (1991)].
11. O'Neill D.M., Lewis C.L.S., Neely D., et al. *Phys. Rev. A*, **44**, 2641 (1991).
12. Springer P.T., Field D.J., Wilson B.G., et al. *Phys. Rev. Lett.*, **69**, 3735 (1992).
13. Chenais-Popovics C., Fajardo M., Gilleron F., et al. *Phys. Rev. E*, **65**, 016413 (2001).
14. Renaudin P., Blancard C., Bruneau J., et al. *J. Quant. Spectr. Rad. Transfer*, **99**, 511 (2006).
15. Perry T.S., Springer P.T., Fields D.F., et al. *Phys. Rev. E*, **54**, 5617 (1996).
16. Bel'kov S.A., Dolgoleva G.V. *Voprosy Atomnoi Nauki i Tekhniki. Ser. Matematicheskoe Modelirovanie Fizicheskikh Protssessov*, **1**, 59 (1992).
17. Annenkov V.I., Bel'kov S.A., Suslov N.A., et al. *J. Phys. IV France*, **133**, 139 (2006).
18. Perry T.S., Davidson S.J., Serduke F.J.D., et al. *Phys. Rev. Lett.*, **67**, 3784 (1991).
19. Chenais-Popovics C., Thais F., Eidmman K., et al. *Proc. Second Int. Conf. «Inertial Fusion Science and Applications»* (Kyoto, Japan, 2001) p.451.
20. Henke B.L., Gullikson E.M., Davis J.C. *At. Data Nucl. Data Tables*, **54**, 181 (1993).
21. Perry T.S., Bedil K.S., Cauble R., et al. *J. Quant. Spectr. Rad. Transfer*, **54**, 317 (1995).
22. Back C.A., Perry T.S., Bach D.R., et al. *J. Quant. Spectr. Rad. Transfer*, **58**, 415 (1997).